PUSH-PULL FATIGUE TESTS
ON DUCTILE AND VERMICULAR CAST IRONS

Cristiano Fragassa[1*] – Roberto Zigulic[2] – Ana Pavlovic[3]

[1]Department of Industrial Engineering, University of Bologna, viale Risorgimento 2, 40136 Bologna, Italy
[2]Faculty of Engineering, University of Rijeka, Vukovarska 58, 51000 Rijeka, Croatia
[3]Interdepartmental Center for Industrial Research on Advanced Applications and Materials, University of Bologna, via Terracini 24, 40131 Bologna, Italy

ARTICLE INFO	Abstract:
	This article aims at measuring and comparing the fatigue strength with fully reversed push-pull tests in the case of two different cast irons: ductile and vermicular. Spheroidal Graphite Iron (SGI), also known as ductile cast iron, is nowadays used in a very large variety of applications. It represents a valid option when strength and stiffness are required, namely, when high values of tensile strength and Young's modulus are coupled with appreciable deformation before failure. By contrast, a different cast iron, known as Compacted Graphite Iron (CGI) or vermicular cast iron, presents its benefits in replacing SGI with respect to specific applications. In particular, with better castability, machinability and thermal resistance, SGI is ideal when components suffer simultaneous mechanical and thermal loadings, such as cylinder blocks and heads. While SGI benefits of a wide scientific literature, CGI is a relatively unknown material, especially referring to its response under fatigue loads.

1 Introduction

1.1 Cast iron

Cast iron is a group of iron-carbon alloys with an amount of carbon content greater than 2% and other elements (as Si, Mn, P, Cr) in lower part.
These constituents affect the microstructure and, as a consequence, the final properties of the cast iron. Moreover, a large variability in properties is evident, depending on the mode the carbon is transformed in graphite [1].
The following cast alloys are identified [2]:

- white cast iron
- grey cast iron
- malleable cast iron
- ductile cast iron
- vermicular cast iron

Essentially, only grey and the ductile cast irons present a significant utilisation [3]. Most of the production of white cast iron is reprocessed for obtaining malleable or ductile cast irons. Nevertheless, the presence of malleable cast iron on the market is declining very fast nowadays since the higher complexity in processing for this alloy is not justified by lower improvements in properties.

---

* Cristiano Fragassa. Tel.: +39.347.6974046 ; fax: +39.051.20.93.412
E-mail address: cristiano.fragassa@unibo.it.

Ductile cast iron offers incredibly high mechanical properties thanks to a spheroidal shape of graphite. The shape is so relevant for the final properties that the material is also known as Spherical Graphite Iron (SGI) or Nodular cast iron [4].

Although grey iron is largely used nowadays, in comparison with ductile cast irons it is mainly limited to marginal applications where the lower costs balance their inferior properties of resistance. However, ductile cast iron is largely preferred when superior mechanical characteristics are requested. It is worth noting that so called Vermicular Graphite Iron or Compacted Graphite Iron (CGI) is considered to be somewhere in the middle between grey and ductile cast irons. Also, in the case of CGI, its peculiarities are directly related to the specific ("vermicular") shape of graphite particles. While grey cast iron is characterized by randomly oriented graphite flakes, as in ductile iron (SGI) graphite exists as individual spheres, in CGI graphite flakes are randomly oriented and elongated as in grey iron, but they are shorter, thicker and with rounded edges, in some aspects more similar to SGI [5]. Micrographs for CGI and SGI are reported in Fig. 1.
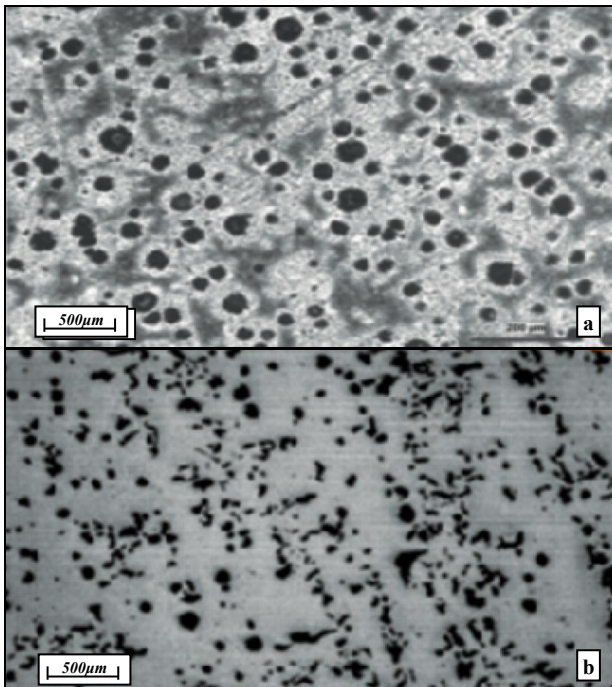

Figure 1. Micrographs: a) grey cast iron; b) ductile iron [14].

1.2 Properties

Several interesting dissertations compare the properties of cast irons, in general [6-8] and either in consideration of specific aspects [9] or applications [10]. Common properties for cast irons are reported in Table 1. It is possible to summarize saying that the technological advantages of SGI are numerous and that they are driving the material toward large success: versatility, high performance, lower cost [11, 12].

Therefore, this research is mainly focused on SGI and CGI.

CGI appeared significantly inferior with respect to SGI [13-15], i.e., twice weaker with less stability in processing. These limits, together with lower familiarity and scarce knowledge on potentialities, reduce its penetration to few practical cases [16].

Table 1. Typical properties of grey, compacted and ductile cast irons [4, 14]

Property		Grey	CGI	SGI
Tensile Strength	MPa	250	368	650
Elastic Modulus	GPa	105	145	160
Poisson's Ratio		0.21	0.22	0.24
Elongation	%	0	1.5	5
Therm. Conductivity	W/mK	48	37	28
Damping Capacity		1	0.35	0.22
Hardness	BHN	190	230	235

2   Methods

2.1 Basic information

In materials science, fatigue refers to weakening of a material caused by repeatedly applied loads. It is the progressive and localized structural damage that occurs when a material is subjected to cyclic loading. The nominal maximum stress values that cause such damage may be much less than the strength of the material typically quoted as the ultimate tensile stress limit, or the yield stress limit. ASTM defines fatigue life as the number of stress cycles of a specified character that a specimen sustains before failure of a specified nature occurs

[17]. For some materials, there is a theoretical value for stress amplitude below which the material will not fail for any number of cycles, called a fatigue limit, endurance limit, or fatigue strength [18].

Generally speaking, engineers use any of three methods to determine the fatigue life of a material: the stress-life method, the strain-life method, and the linear-elastic fracture mechanics method [19]. In this investigation the stress-life method is applied. In [20] the effects of graphite shape on thermal fatigue resistance of cast iron is investigated, while [21] proposes a model for predicting the fatigue life and compares these predictions with experiments.

For the sake of completeness, it is also possible to list an additional procedure for the determination of the fatigue life, the so called Uniform Material Law (UML). This method was developed for fatigue life prediction of aluminum and titanium alloys [22], extended to high-strength steels [23] and, recently, to cast iron [24].

2.2 S-N curve

In high-cycle fatigue situations, materials performance is commonly determined by the preliminary evaluation of an S-N curve, also known as a Wöhler curve. This is frequently expressed as a graph of the magnitude of a cyclic stress (S) against the logarithmic scale of cycles to failure (N). In stress-life, S-N curves are derived from tests on samples of the material to be characterized where a regular sinusoidal stress is applied by a testing machine which also counts the number of cycles to failure. Tests are realized at various stress (S) levels recording the cycles before failure (N). Each test generates a point on the S—N plot though in some cases there is a runout where the time to failure exceeds that one available for the test (censoring). Analysis of fatigue data requires techniques from statistics, especially survival analysis and linear regression [25].

2.3 Standards

In order to evaluate the fatigue beaviour of the cast irons under investigation, CGI and SGI specimens were subjected to these fatigue experimental tests according to the ISO 12107. This International Standard rules the testing of metallic materials with respect to fatigue loads and also proposes a statistical method for the analysis of experimental measures [26]. Another purpose of ISO 12107 is to permit to determine the fatigue properties with a high degree of confidence and, at the same time, by using an acceptable number of specimens. With this scope, it proposes a way to analyse the fatigue life properties at a variety of stress levels using a relationship that can linearly approximate the material response in appropriate coordinates. It estimates the S-N curve, including finite and infinite fatigue life ranges, by a reasonable number of specimens. For this scope, it assumes that the S-N curve consists of an inclined straight line in the finite fatigue life range and a horizontal straight line in the infinite fatigue life regime. This simplification is often realistic for many engineering materials, when the data are represented using appropriate coordinates, generally on semi-log or log-log paper.

2.4 Consistency of sample

The reliability of test results is primarily dependent on the number of specimens tested. It increases with the number of tests. The total number of specimens required may be determined by reference to the typical values, taking into account the purpose of the test and the availability of test material.

The number of specimens allocated to each line is determined in a way that permits the fatigue strengths predicted by each, at their point of intersection, to have equal statistical confidence.

In general, the following relationship is suggested:

$$\frac{n_2}{n_1} = \frac{l+1}{2l-1} \tag{1}$$

where n_1 and n_2 are the number of tests for the inclined line and the horizontal line, respectively, and l is the number of stress levels for testing along the inclined line. A few extra specimens were kept in reserve, because tests may not always take place as expected. Having extra specimens available may help resolve such unexpected problems.

The ISO 12107 test requires at least 14 specimens, therefore 8 is used for estimating the S-N curve in the finite fatigue life range (inclined line) and another 6 specimens for the fatigue strength at the infinite fatigue life regime (horizontal line). In Fig. 2 this concept is presented.
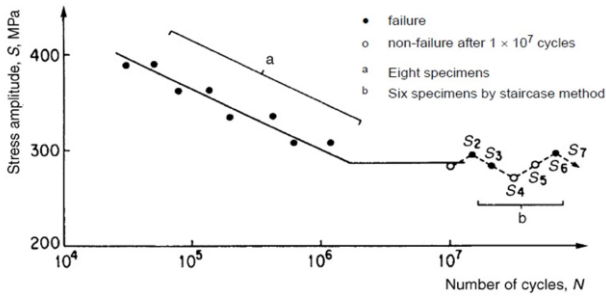
Figure 2. Model of combined method for the S-N curve with 14 specimens [26].

2.5 Sequence of tests

The experimental fatigue strength characterization was performed by fully reversed push-pull tests (equivalent to a stress ratio constantly equal to -1). Tests were realized at different stresses (S), but the sequence of loads can be defined using the so called "staircase method". It is necessary to have rough estimates of the mean and the standard deviation of the fatigue strength for the materials. Start the test at a stress level close to the estimated mean strength. Select a stress step preferably close to the standard deviation (if unknown, use a step of about 5% of fatigue strength). Test a first specimen, randomly chosen, at the first stress level to find if it fails before the given number of cycles. For the next specimen, also randomly chosen, increase the stress level by a step if the preceding specimen did not fail, and decrease the stress by the same amount if it failed. Continue testing until all the specimens have been tested in this way (Fig. 3).

A "modified staircase" method with fewer specimens is possible if the standard deviation is known and only the mean of the fatigue strength needs to be estimated. Conduct tests as in the staircase method changing the stress by a fixed step depending on whether the preceding event was a failure or non-failure, respectively.

Figure 3. An example of „staircase" method [26].

3 Experimental investigation

3.1 Equipment

Fatigue tests were realized using a RUMUL MIKROTRON resonant testing machine. The excitation system consists of an elasticity system combined and an electro magnet. There are both integrated in the dynamic load flow and work combined [27]. This technical solution permit loads of 20 kN up to 250 Hz of frequency. The exact value depends on specimens' stiffness and activated mass. Specimens are placed in the clamps vertically and tested by push-pull controlled movements. Figure 4 reports the shape and dimension for specimens. Measures were very precise, with a control accuracy of 0.5%.
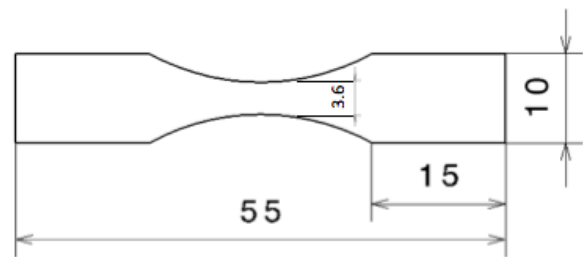

Figure 4. Geometry of the specimen (in mm).

3.2 Material

Specimens were extracted from CGI and SGI cast plates realized in sand casting (Fig. 5).
Specifically, a plate in SGI and, just after, a plate in CGI were cast. They were realized inside the same process and using, as a base, the same melting alloy, but modifying the composition by inclusion of additives. In practice, specific and different additives were directly introduced into the furnace to produce SGI or CGI. In the case of SGI castings, before the pouring, the melt (with a sulphur content lower than 0.01% wt.) was inoculated by adding ferrosilicon alloys and modified with Fe-Si-Mg master alloys. In the production of CGI castings also Ti was added. Special attentions were adopted to keep unchanged the other process conditions, passing from SGI to CGI, and, in particular, the same pouring temperature, fixed at 1400°C.
The chemical composition is reported in Table 2. Further details regarding the main conditions used during the casting process and the geometry of casts

(including the specific zones where samples were excavated from), together with a comparative analysis of microstructure, porosity, fracture surfaces of the two alloys are reported in [14, 15]. Specimens were machined in shape according to the EN 1563. This standard [28] outlines legal and regulatory requirements providing ways to classify SGI on the base of quality, hardness and other mechanical properties.

Figure 5. Production of specimens by sand casting: withdrawing a sample for tests on the molten metal.

Table 2. Chemical composition of specimens (%)

%	C	Si	Mn	P	S	Ni
SGI	3.63	2.65	0.276	0.036	0.002	0.06
CGI	3.63	2.57	0.272	0.034	0.005	0.06
	Cr	Cu	Mg	Sn	Ti	Al
SGI	0.083	0.077	0.049	0.011	0.033	0.011
CGI	0.082	0.075	0.012	0.011	0.074	0.011

3.3 Samples

In accordance with ISO 12107, tests were realized at various stress levels in order to determine the mean S-N curve and giving a probability of failure (P_F) lower than 50%. It is assumed that the variation in the logarithm of the fatigue life follows a normal distribution with constant variance as a function of stress. Since it was at the presence of ordinary high-cycle fatigue tests, the stress levels was chosen in the way that the resultant fatigue lives would have had a spread of two decades of cycles, e.g. from 5×10^4 to 1×10^6 cycles. Table 3 gives some typical figures for the number of specimens. A confidence

level equal or higher than 95% is generally only used for reliability design purposes. Conversely, the 50% confidence level is adopted for exploratory tests. All the others in between are used for general engineering purposes. In this specific explorative study, 16 specimens of each materials were used, 8 for the Wöhler's curve estimation and 8 for the staircase method. This choice, in line with the ISO 12107 specification, is equivalent to a probability of failure (P_F) of 10% and a confidence level ($1-\alpha$) higher than 50%.

Table 3. Minimal number of specimens for the given levels of probability of failure and confidence [26]
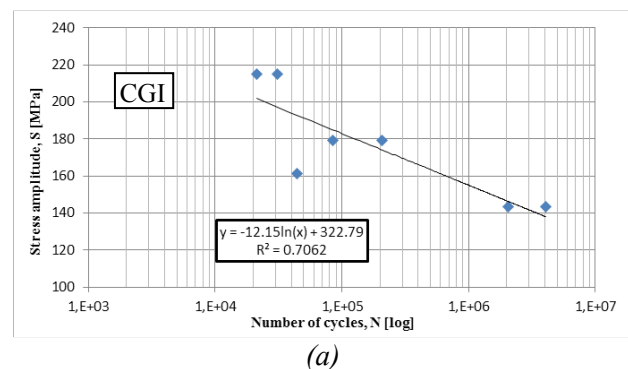
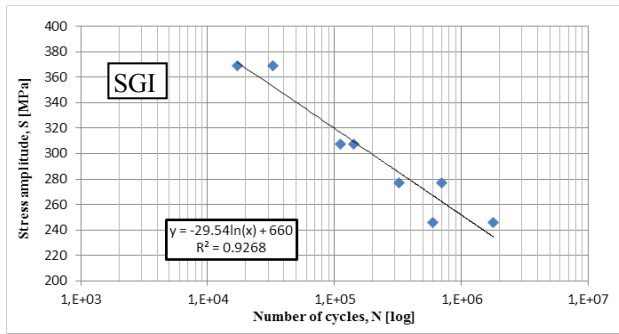| Probability of Failure P_F (%)	Number of specimens		
	Confidence level, $1-\alpha$ (%)		
	50	90	99
50	1	3	4
10	7	22	28
5	13	45	58
1	69	229	298

3.4 High cycle fatigue

The estimation of the Wöhler's slope (inclined line) for CGI and SGI is reported in Fig. 6: the line was evaluated in Excel by a simple regression method. It represents the (low-high cycle) fatigue in finite fatigue regions (valid for P_F =10% and ($1-\alpha$)>50%). Wöhler's curve gradient follows up the trendline's slope according to the next relations:

$$S_{CGI} = -12.15 \ln(N) + 372.79 \quad [\text{MPa}] \quad (2)$$

$$S_{SGI} = -29.54 \ln(N) + 660 \quad [\text{MPa}] \quad (3)$$

(a)

(b)

Figure 6. Wöhler's curve analyses in the case of CGI (a) and SGI (b).

or, expressed in terms of power laws:

$$S_{CGI} = 402.94 \cdot N^{-0.0698} \quad [MPa] \quad (4)$$

$$S_{SGI} = 960.74 \cdot N^{-0.0965} \quad [MPa] \quad (5)$$

3.5 Fatigue limit

The fatigue strength in the infinite fatigue life range (horizontal part) is estimated, as already said, in accordance with the modified staircase method, as detailed in ISO 12107: 2012, Annex A.2 [26]. Specimens are tested sequentially under decreasing stresses, improving the cycles, until a failure occurs. Further examples of the application of the modified staircase method, as procedure for optimizing fatigue experiments are available in [29].

In Fig. 7 results from specimens of CGI and SGI, tested in infinite fatigue regions in accordance with the staircase method are shown.

The failure is, therefore, the only event considered in the analysis (no censures). This procedure is used, in practice, in order to estimate the lower limit of the fatigue life for 10% probability of failure, at a confidence level of 50% $\widehat{S}_{(10,50)}$.

Further steps of calculations are necessary before obtaining these results, as described below.

Firstly, an appropriate sequel of stress levels has to be defined for both materials. Only 3 stress levels (S_0, S_1, S_2) were considered and the highest one (S_2) was set as coincident with the lowest stress measured during the previous high-cycle tests (equal to 143 MPa for CGI and 246 MPa for SGI).

The same experimental results were also used for an estimation of the Standard Deviation (equal to, respectively, d_{CGI}=18 MPa and d_{SGI}=31 MPa).

In Table 4, the value of stresses, S_i [MPa], related to each specific *i-th* level of testing and the number of failure events, f_i, occurred in that level are given. It is noteworthy that each level increases the previous one in stress intensity, for a standard deviation, *d* (18 MPa for CGI or 31 MPa for SGI).

In Table 5 the intermediate constants *A*, *B*, *C* and *D* are also evaluated according to the ISO standard.
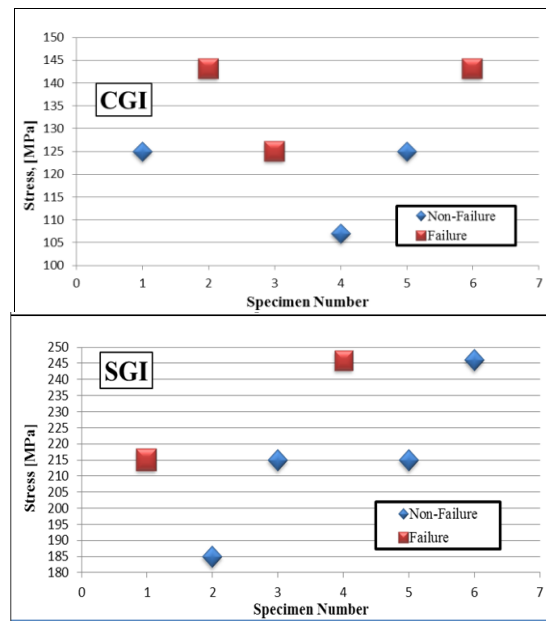

Figure 7. Specimens tested with staircase method in the case of CGI (up) and SGI (down).

Table 4. Analysis of the staircase data

CGI				
Stress S_i MPa	**Level *i***	f_i	if_i	$i^2 f_{i_i}$
143	2	2	4	8
125	1	1	1	1
107	0	0	0	0
Total	-	3	5	9

SGI				
Stress S_i MPa	**Level *i***	f_i	if_i	$i^2 f_{i_i}$
246	2	1	2	4
216	1	1	1	1
185	0	0	0	0
Total	-	2	3	5

Table 5. Evaluation of the constants A, B, C and D according to ISO standard

Formula	CGI	SGI
$A = \sum_{i=1}^{l} i f_i$	5	3
$B = \sum_{i=1}^{l} i^2 f_i$	9	5
$C = \sum_{i=1}^{l} f_i$	3	2
$D = \dfrac{BC - A^2}{C^2}$	0.22	0.25

The lower limit of fatigue life $\widehat{S}_{(P,1-\alpha,v)}$ depends on:

- the mean fatigue strength $(\hat{\mu}_y)$;
- the estimated standard deviation for the logarithm of the fatigue life $(\hat{\sigma}_y)$;
- the coefficient for the one-sided tolerance limit for a normal distribution $(k_{(P,1-\alpha,v)})$.

These values can be expressed and calculated as:

$$\widehat{S}_{(P,1-\alpha,v)} = \hat{u}_y - k_{(P,1-\alpha,v)} \cdot \widehat{\sigma}_y \qquad (6)$$

$$\hat{u}_y = S_0 + d\left(\frac{A}{C} + \frac{1}{2}\right) \qquad (7)$$

$$\widehat{\sigma}_y = 1.62 \cdot d(D + 0.029) \qquad (8)$$

Adding, $k_{(P,1-\alpha,v)}$ is given in Table 6 considering that $v = 5$ as a number of degrees of freedom, calculated by subtracting from the total number of observations the number of parameters estimated from the data.
In accordance with the standard recommendation of $v = n - 1$, where n is the number of items in a population, equal to 6.
$k_{(P,1-\alpha,v)}$ has the same value for both materials. In particular, considering, also in this case, a desired probability of $P_F = 10\%$ and a confidence level $1 - \alpha = 90\%$, then, finally,

$$k_{(P,1-\alpha,v)} = 2.494 \qquad (9)$$

As a consequence, in the case of CGI:

$$\hat{u}_y = 107 + 18\left(\frac{5}{3} + \frac{1}{2}\right) = 146 \qquad (10)$$

$$\widehat{\sigma}_y = 1.62 \cdot 18(0.222 + 0.029) = 7.32 \qquad (11)$$

$$\widehat{S}_{(P,1-\alpha)} = 146 - 2.494 \cdot 7.32 = 128 \, \text{MPa} \qquad (12)$$

while, for SGI, is:

$$\hat{u}_y = 185 + 31\left(\frac{3}{2} + \frac{1}{2}\right) = 247 \qquad (13)$$

$$\widehat{\sigma}_y = 1.62 \cdot 31(0.25 + 0.029) = 14.01 \qquad (14)$$

$$\widehat{S}_{(P,1-\alpha)} = 247 - 2.494 \cdot 14.01 = 212 \, \text{MPa} \qquad (15)$$
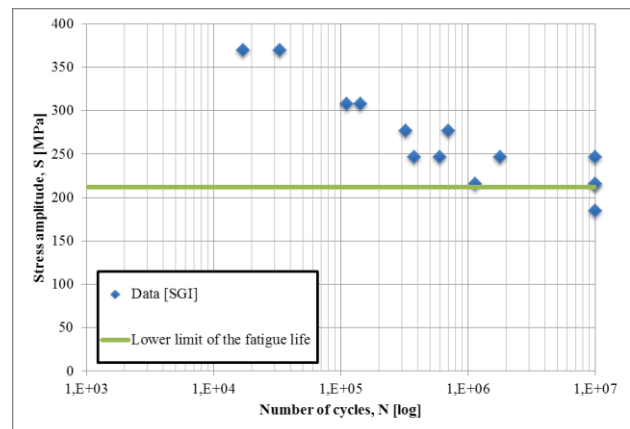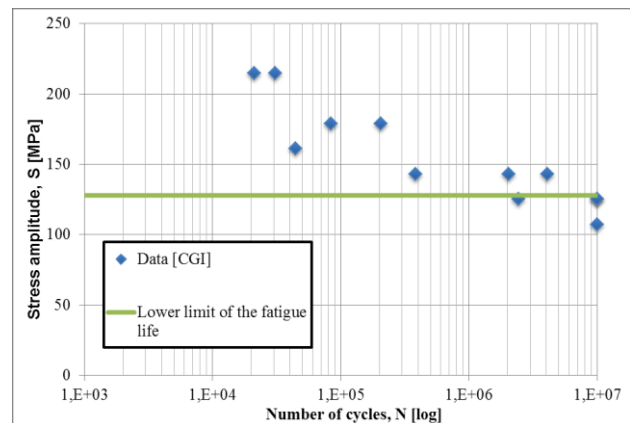

Figure 8. Distribution of fatigue strength, S-N curves, and lower limit of the fatigue life.

Figure 8 displays the S-N curves and the lower limit of the fatigue life for both materials.

4   Results and discussion

4.1 Experimental evidences

The fatigue test required 16 specimens for each of the two materials under investigation. Between them, 8 ones were used for estimating the *S-N* curve in the finite fatigue life range (inclined line) and 8 for the fatigue strength at the infinite fatigue life regime (horizontal line). The exact number of cycles that specimens hold out before failure or censure is shown in Tables 7. In this table, loads are expressed in terms of % of the Ultimate Tensile Stress (UTS).

The complete S-N curves for both materials, showing the values of applied loads against the number of cycles which specimen endured before the failure and in the moment of failure are shown in Fig. 9. It could be seen that 4 specimens of CGI and 4 specimens of SGI passed 10^7 cycles without failure. These censored data were considered in the estimation and in accordance with the statistical procedures detailed in [30].

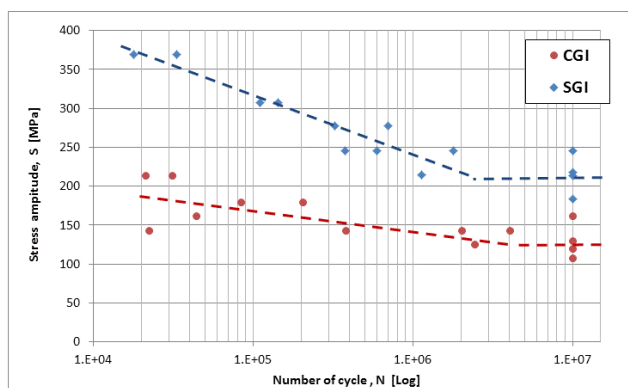The chart also displays lower limit of the fatigue life.

Figure 9. Comparing the fatigue behaviour of CGI and SGI.

In particular, it is reported how CGI offers a lower resistance to fatigue loads with respect to SGI, as -40% in terms of fatigue limits (212 vs 128 MPa). But it is also evident how CGI seems less affected by fatigue phenomena (detectable by lower grade of inclined lines). In particular, using a linear extrapolation of the inclined lines as valid method

for describing the behaviour of the two materials in the low cycle fatigue region ($<2\cdot10^4$ cycles), it is possible to estimate the values of 200 MPa and 400 MPa as the stress amplitude of CGI and SGI at 10^4 cycles. It also means, as a consequence / consequently, that SGI faces a reduction in fatigue strength of -47%, higher than CGI's -36%.

4.2 Additional note

Specimens were allocated to individual fatigue tests, in principle, in a random way, in order to minimize unexpected statistical bias. The order of testing of the specimens was also randomized in a series of fatigue tests. In Table 7 specimens are reported according to sequence testing criteria.

Additionally, each test series were carried out at equal rates of progress and testing was completed at approximately the same time.

Fatigue test results usually display significant scatter despite that the tests are carefully conducted to minimize experimental error. A component of this variation is due, between other phenomena, to inequalities related to chemical composition or heat treatment, among the specimens. At the moment, this specific risk was only reduced by extracting specimens from the same castings and in adjacent positions. Further experimental sessions will be realized with the scope to investigate these aspects. In this case, a larger number of specimens will be preferred.

Figure 10. SEM micrographs on the fracture surfaces of SGI (left) and CGI (right) specimens.

Moreover, mechanical properties of cast iron are strongly related to different microstructures (e.g. grade of nodularity, grade of perlit) or to the specific mechanisms of failure. A deep analysis of these complex aspects, also comparing CGI and SGI, is reported in [14, 15, 31] where it is noted that, for instance, the fracture surfaces (Fig. 10)

show cleavage as the dominant fracture mechanism. At the same time, CGI shows higher decohesion at the matrix-graphite interface resulting in lower ductility. In fact, in CGI specimens, cleavage planes are wider and with very high decohesion at the matrix-graphite interface.

5 Conclusion

Mechanical, physical and manufacturing properties of cast iron make it attractive for many fields of application [32], even when material defects are considered [33]. As in design of all metals, fatigue life prediction is an intrinsic and relevant part of the design process of structural sections that are made of cast iron [34] [35]. In this analysis, experimental measures were realized with the aim at investigating the fatigue behaviour of two families of cast alloys: Spheroidal Graphite Iron (SGI) and Compacted Graphite Iron (CGI). The fatigue properties of these cast irons were determined by testing a set of specimens at various stress levels to generate a fatigue life relationship as a function of stress. Tests were performed in fully reverse configuration by a resonance load machine. The results were expressed as an S-N curve that fits the experimental data plotted in appropriate coordinates together with the determination of the lower limit of fatigue life.

Information on fatigue behaviour is particularly relevant for these materials. SGI is largely known, both at the scientific levels and industrial use. Besides, CGI is a relatively unused and unknown material since its mechanical properties are positioned in the middle between the excellent SGI and the less performing white, grey and malleable irons. With respect to these more traditional cast irons, the production of CGI presents higher cost and more difficulties. At the same time CGI could represent the perfect choice with respect to specific technical needs when SGI is not applicable while the all other cast irons presents that resistances is too low.

During this investigation, standard test methods were used and validated as a way for the determination of fatigue parameters in industrial environment. It is known, and highlighted during the experiment, that the results of fatigue tests display significant variations even when the test is controlled very accurately. In general, these variations could be attributable, in part, to non-uniformity of test specimens. But not in this case:

slight differences in chemical composition, heat treatment, surface finish were all adequately prevented considering their relevance [36]. The residual non-uniformity is related to the stochastic process of fatigue failure itself that is intrinsic to metallic engineering materials. A larger number of specimens will be used for further investigations.

Finally, another campaign for investigating the fatigue behavior of cast irons has been launched, in parallel, by experiments on rotating bending fatigue. By extending and comparing all results, it will be possible to enlarge the level of knowledge on SGI and, more relevantly, CGI.

6 Acknowledgement

References

[1] Shackelford, J. F., William, A.: *CRC materials science and engineering handbook*, CRC press, FL, USA, 2000.

[2] Campbell, F.C.: *Elements of metallurgy and engineering alloys*. ASM International, Materials Park, Ohio, 2008.

[3] Mi, G., Li, C., Gao Z.: *Application of numerical simulation on cast-steel toothed plate*, Engineering Review, 34 (2014), 1.

[4] Tiedje, N. S.: *Solidification, processing and properties of ductile cast iron*, Materials Science and Technology, 26 (2010), 5, 505-514.

[5] Dawson, S., Schroeder T.: *Compacted graphite iron – a viable alternative. Engineered casting solutions.* AFS Translation, Spring, 2000.

[6] Angus, H. T.: *Cast iron: physical and engineering properties*, Elsevier, 2013.

[7] Elliott, R.: *Cast iron technology*, Butterworth-Heinemann, Oxford, 1988.

[8] Davis, J. R. (ed.): *Speciality handbook: cast irons*. ASM International Materials Park, USA, 1996, 33-267.

[9] Lampman, S.: *Fatigue and fracture properties of cast irons*. ASM International, Materials Park, USA, 1996, 665-679.

[10] Baicchi, P., Collini, L., Riva, E.: *A methodology for the fatigue design of notched castings in grey cast iron.* Engineering Fracture Mechanics, 74 (2007), 4, 539-548.

[11] Fatahalla, N., Bahi, S., Hussein, O.: *Metallurgical parameters, mechanical properties and machinability of ductile cast iron*, Journal of Materials Science, 31 (1996), 21, 5765-5772.

[12] James, M. N., Wenfong, L.: *Fatigue crack growth in austempered ductile and grey cast irons—stress ratio effects in air and mine water*, Materials Science and Engineering, 265 (1999), 1, 129-139.

[13] Radovic, N., Morri, A., Fragassa, C.: *A study on the tensile behaviour of spheroidal and compacted graphite cast irons based on microstructural analysis*, Proceedings of the 11th IMEKO TC15 Youth Symposium Experimental Solid Mechanics, Brasov, Romania, 2012, 185-190.

[14] Fragassa, C., Radovic, N., Pavlovic, A. Minak, G.: *Comparison of mechanical properties in compacted and spheroidal graphite irons*. Tribology in Industry, 38 (2016), 1, 49-59.

[15] Fragassa, C., Minak G., Pavlovic, A.: *Tribological aspects of cast iron investigated via fracture toughness*, Tribology in Industry, 38 (2016), 1, 1-10.

[16] Dawson, S., Schroeder, T.: *Practical applications for compacted graphite iron,* AFS Transactions, 47 (2004), 5, 1-9.

[17] Stephens, R. I., Fuchs, H. O.: *Metal Fatigue in Engineering (Second ed.)*. John Wiley & Sons, Inc. 69, 2001

[18] Bathias, C.: *There is no infinite fatigue life in metallic materials*, Fatigue & Fracture of Engineering Materials & Structures 22 (1999), 7, 559–565.

[19] Shigley, J. E., Mischke, C. R.: *Machine design.* McGraw-Hill, New York, 1956.

[20] Tong, Xin, Zhou, Hong, Ren, Lu-quan, et al.: *Effects of graphite shape on thermal fatigue resistance of cast iron with biomimetic non-smooth surface*, International Journal of Fatigue 31 (2009), 4, 668-677.

[21] Seifert, T., Maier, G., Uihlein, A., et al.: *Mechanism-based thermomechanical fatigue life prediction of cast iron. Part II: Comparison of model predictions with experiments*, International Journal of Fatigue 32 (2010), 8, 1368-1377.

[22] Bäumel, A., Seeger, T.: *Materials data for cyclic loading, supplement 1*, Elsevier, 1990.

[23] Korkmaz, S.: *Uniform material law: Extension to high-strength steels,* VDM, 2010.

[24] Korkmaz, S.: *A methodology to predict fatigue life of cast iron: Uniform material law for cast iron,* Journal of Iron and Steel Research, International 18 (2011), 8.

[25] Bozic, Z., Braut, S.: *Effect of secondary bending on fatigue crack growth in stiffened panels*, Engineering Review, 30 (2010), 1.

[26] ISO 12107:2012. *Metallic materials — Fatigue testing — Statistical planning and analysis of data.*

[27] Rumul Mikrotron, accessed on 10.12.2015 at: http://www.rumul.ch/pdf/mikrotron_e.pdf

[28] EN 1563:2012. *Founding. Spheroidal graphite cast iron.*

[29] Hück M.: *Ein verbessertes Verfahren zur Auswertung von Treppenstufenversuchen*, Z. Werkstofftcchnik 14 (1983), 17.

[30] Minak, G., Morelli, P. Zucchelli, A.: *Fatigue residual strength of circular laminate graphite–epoxy composite plates damaged by transverse load.* Composites Science and Technology, 69 (2009), 1358–1363.

[31] Fragassa, C, Pavlovic, A. *Compacted and Spheroidal graphite irons: experimental evaluation of Poisson's ratio,* FME Translation, 44 (2016), 4 (to be published).

[32] Kolic, D., Fafandjel, N., Bicanic, D.: *Proposal for the determination of technological parameters for design rationalization of a shipbuilding production program*, Engineering Review, 30 (2010), 2.

[33] Khaira, A., Srivastava, S., Suhane, A.: *Analysis of relation between ultrasonic testing and microstructure: a step towards highly reliable fault detection,* Engineering Review, 35 (2015), 2.

[34] Mi, G., Li, C., Liu, Y., Zhang, B., Song G.: *Numerical simulation and optimization of the casting process of a cast-steel wheel,* Engineering Review, 33 (2013), 2.

[35] Mi, G., Li, C., Chen, L., Xu, L.: *Numerical simulation and process optimization on cast steel bearing sleeve*, Engineering Review, 35 (2015), 1.

[36] Radenovic, A., Malina, J., Matijasic, G.: *The change in surface area properties of blast furnace sludge treated by citric acid*, Engineering Review, 33 (2013), 1.

[37] SCM Foundry, accessed on 10.12.2015 at: http://www.scmfonderie.it/?l=en&p=azienda

Appendix

Table 6. Statistical table for coefficient $k_{(P,1-\alpha,\nu)}$ estimation

Number of degrees of freedom ν	Probability P_F (%)							
	10		5		1		0.1	
	Confidence level, $1-\alpha$ (%)							
	90	95	90	95	90	95	90	95
2	4.258	6.158	5.310	7.655	7.340	10.550	9.651	13.860
3	3.187	4.163	3.957	5.145	5.437	7.042	7.128	9.215
4	2.742	3.407	3.400	4.202	4.666	5.741	6.112	7.501
5	2.494	3.006	3.091	3.707	4.242	5.062	5.556	6.612
6	2.333	2.755	2.894	3.399	3.972	4.641	5.301	6.061
7	2.219	2.582	2.755	3.188	3.783	4.353	4.955	5.686
8	2.133	2.454	2.649	3.031	3.641	4.143	4.772	5.414
9	2.065	2.355	2.568	2.911	3.532	3.981	4.629	5.203
10	2.012	2.275	2.503	2.815	3.444	3.852	4.515	5.036

Table 7. Values of all loads and all numbers of cycles, CGI and SGI specimens

	spec:	Number of Cycles		Loads			
		N_{min}	N_{max}	UTS (MPa)	[%]	Stress [MPa]	Failure
CGI	A2	21200	21700	358	60	214	*
	A3	84300	84800	358	50	179	*
	A4	4083000	4085200	358	40	143	*
	A5	31000	31600	358	60	214	*
	A6	206400	207100	358	50	179	*
	A7	2038000	2039200	358	40	143	*
	A8	10000000	10000000	358	45	161	
	A9	44200	44800	358	45	161	*
	A10	10000000	10000000	358	35	125	
	A11	381800	382600	358	40	143	*
	A12	2446700	2447000	358	35	125	*
	A13	10000000	10000000	358	30	107	
	A14	10000000	10000000	358	35	125	
	A15	22100	22900	358	40	143	*

| | spec: | Number of Cycles | | Loads | | | |
		N_{min}	N_{max}	UTS (MPa)	[%]	Stress [MPa]	Failure
SGI	B3	17100	19000	615	60	369	*
	B4	142500	143600	615	50	307	*
	B5	600400	601300	615	40	246	*
	B8	33000	33900	615	60	369	*
	B7	111100	112100	615	50	307	*
	B6	1795500	1796600	615	40	246	*
	B9	701400	702300	615	45	277	*
	B10	325200	326100	615	45	277	*
	B11	1133000	1134500	615	35	215	*
	B12	10000000	10000000	615	30	184	
	B13	10000000	10000000	615	35	215	
	B14	377400	378200	615	40	246	*
	B15	10000000	10000000	615	35	215	
	B16	10000000	10000000	615	40	246	